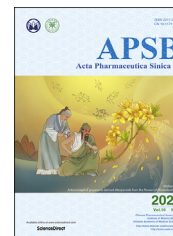




Chinese Pharmaceutical Association  
Institute of Materia Medica, Chinese Academy of Medical Sciences

Acta Pharmaceutica Sinica B

[www.elsevier.com/locate/apsb](http://www.elsevier.com/locate/apsb)  
[www.sciencedirect.com](http://www.sciencedirect.com)



ORIGINAL ARTICLE

# Antinociceptive grayanane-derived diterpenoids from flowers of *Rhododendron molle*



Yong Li, Yuxun Zhu, Zhaoxin Zhang, Li Li, Yunbao Liu, Jing Qu, Shuanggang Ma, Shishan Yu\*

State Key Laboratory of Bioactive Substance and Function of Natural Medicines, Institute of Materia Medica, Chinese Academy of Medical Sciences & Peking Union Medical College, Beijing 100050, China

Received 25 July 2019; received in revised form 23 August 2019; accepted 24 October 2019

## KEY WORDS

*Rhododendron molle*;  
Diterpenoid;  
Grayanane;  
Dimeric;  
Antinociceptive;  
Analgesic

**Abstract** Twelve new grayanoids (**1–12**) along with five known compounds were isolated from flowers of *Rhododendron molle*. Their structures were fully characterized using a combination of spectroscopic analyses, computational calculations, and single crystal X-ray diffraction. Rhomollone A (**1**) possesses an unprecedented 5/6/6/5 tetra-cyclic ring system (B-*nor* grayanane) incorporating a cyclopentene-1,3-dione scaffold. Rhodomollein XLIII (**2**) is a dimeric grayanoid, containing a novel 14-membered heterocyclic ring with a  $C_2$  symmetry axis. The antinociceptive activities of compounds **3**, **4**, **6**, **7**, and **12–17** were evaluated by an acetic acid-induced writhing test. Among them, compounds **3**, **7**, **12**, **15** and **16** displayed significant antinociceptive activities at a dose of 20 mg/kg with inhibition rates ranging from 41.9% to 91.6%. Compounds **6** and **13** inhibited 46.0% and 39.4% of the acetic acid-induced writhes at a dose of 2 mg/kg, while compound **17** inhibited 34.3% of the writhes at a dose of 0.4 mg/kg.

© 2020 Chinese Pharmaceutical Association and Institute of Materia Medica, Chinese Academy of Medical Sciences. Production and hosting by Elsevier B.V. This is an open access article under the CC BY-NC-ND license (<http://creativecommons.org/licenses/by-nc-nd/4.0/>).

\*Corresponding author. Tel./fax: +86 10 83162679.

E-mail address: [yushishan@imm.ac.cn](mailto:yushishan@imm.ac.cn) (Shishan Yu).

Peer review under responsibility of Institute of Materia Medica, Chinese Academy of Medical Sciences and Chinese Pharmaceutical Association.

<https://doi.org/10.1016/j.apsb.2019.10.013>

2211-3835 © 2020 Chinese Pharmaceutical Association and Institute of Materia Medica, Chinese Academy of Medical Sciences. Production and hosting by Elsevier B.V. This is an open access article under the CC BY-NC-ND license (<http://creativecommons.org/licenses/by-nc-nd/4.0/>).

## 1. Introduction

The flowers of *Rhododendron molle* (naoyanghua) have a long history of application in China and are still used for the alleviation of rheumatism arthralgia, migraine headache, and other pain symptoms<sup>1</sup>. Our previous investigations have revealed several grayanane-type diterpenoids from the roots of *R. molle*, exhibiting highly potent antinociceptive activity<sup>2</sup>. *R. molle* has been regarded as a prolific source of grayanane and related diterpenoids<sup>3</sup>. Recently, we have reported studies on the chemical composition of the roots and fruits of *R. molle* in a series of papers, revealing the occurrence of new grayanane-related carbon skeletons, such as 1,10:2,3-disecograyanane<sup>4</sup>, mollane (*C-nor-D-homo-grayanane*)<sup>5</sup>, and rhodomollane (*D-homo-grayanane*)<sup>6</sup>. Furthermore, Yao et al.<sup>7–9</sup> have also discovered *C-nor-grayanane*<sup>7</sup>, 2,3:5,6-disecograyanane<sup>8</sup>, and mollebenzylane<sup>9</sup> from the leaves of this herb.

In our continuing efforts to identify structurally unique and biologically interesting diterpenoids from rhododendrons, 17 compounds (Fig. 1), including rhomollone A (**1**), which is a grayanane-derived norditerpenoid with a novel 5/6/6/5-fused ring system incorporating a cyclopentene-1,3-dione scaffold, and rhodomollein XLIII (**2**), which is a dimeric grayanoid with a C<sub>2</sub> symmetry axis containing a novel 14-membered heterocyclic ring, were obtained from the flowers of *R. molle*, collected in Guangxi province, China. Herein, we report the isolation, structural elucidation, and bioactivity of the compounds as well as a plausible biosynthetic pathway for **1**.

## 2. Results and discussion

Rhomollone A (**1**), [ $\alpha$ ]<sub>D</sub><sup>20</sup> –5.0 (*c* 0.1, MeOH), was isolated as a white powder. Its molecular formula, C<sub>19</sub>H<sub>26</sub>O<sub>5</sub>, was established by HR-ESIMS: *m/z* 357.1676, Calcd. for [M+Na]<sup>+</sup> 357.1672,

**Table 1** NMR data for compounds **1** and **2** in C<sub>5</sub>D<sub>5</sub>N (*J* in Hz)<sup>a</sup>.

No.	$\delta_{\text{H}}$	$\delta_{\text{C}}$	No.	$\delta_{\text{H}}$	$\delta_{\text{C}}$
1	—	157.0	1/1'	2.96 (brs)	59.4
2	—	154.4	2/2'	5.02 (brs)	84.6
3	—	207.2	3/3'	4.07 (d, 4.5)	86.7
4	—	47.8	4/4'	—	52.1
5	—	206.4	5/5'	—	85.5
7	2.13 (d, 18.5)	27.6	6/6'	4.59 (m)	76.1
	3.74 (d, 18.5)				
8	—	49.0	7/7'	2.28 (m)	45.1
				2.80 (dd, 5.6, 14.0)	
9	1.78 (m)	53.6	8/8'	—	51.8
10	—	70.1	9/9'	2.28 (m)	55.9
11	1.72 (m)	19.3	10/10'	—	77.3
	2.02 (m)				
12	1.79 (m)	27.3	11/11'	1.62 (m)	22.5
	2.46 (m)			1.86 (dd, 14.5, 6.3)	
13	2.46 (m)	55.3	12/12'	1.49 (m)	26.5
				2.51 (m)	
14	5.02 (d, 3.0)	77.0	13/13'	—	51.6
15	1.98 (d, 14.4)	54.5	14/14'	5.57 (s)	81.8
	2.37 (d, 14.4)				
16	—	80.4	15/15'	2.26 (s)	62.5
17	1.60 (s)	24.6	16/16'	—	79.4
18	1.20 (s)	20.8	17/17'	1.45 (s)	23.4
19	0.91 (s)	20.1	18/18'	1.96 (s)	23.7
20	1.83 (s)	27.5	19/19'	1.70 (s)	22.1
			20/20'	1.91 (s)	28.7

<sup>a</sup>Measured at 500 (<sup>1</sup>H) and 125 (<sup>13</sup>C) MHz. —Not applicable.

indicating seven degrees of unsaturation. The IR spectrum suggests the presence of a hydroxy group (3256 cm<sup>-1</sup>) and  $\alpha,\beta$ -unsaturated ketone (1689 cm<sup>-1</sup>) groups in **1**. The <sup>1</sup>H NMR data (C<sub>5</sub>D<sub>5</sub>N, Table 1) of **1** display diagnostic signals for four tertiary methyls ( $\delta_{\text{H}}$  0.91,

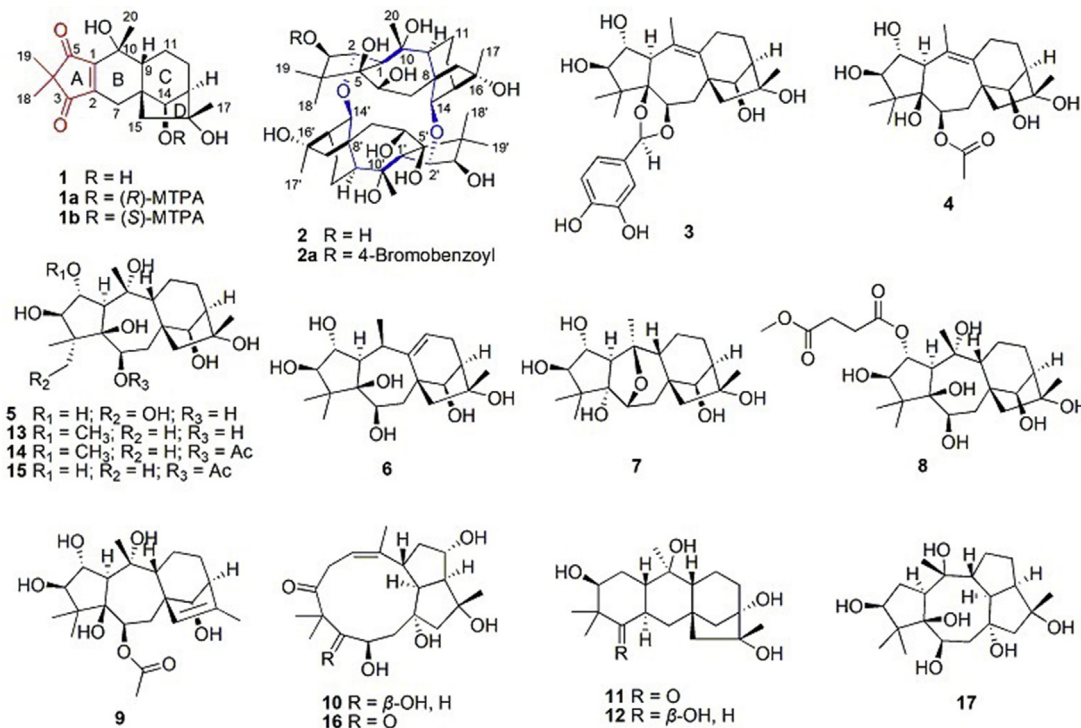


**Figure 1** Structures of compounds **1–17** isolated from flowers of *R. molle*.

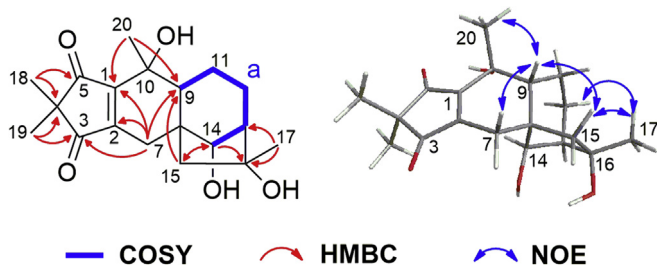
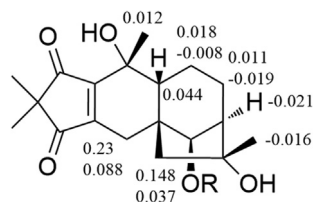


**Figure 2** Selected  $^1\text{H}$ – $^1\text{H}$  COSY, HMBC, and NOE correlations for compound **1**.



**1a** R = (*R*)-MTPA

**1b** R = (*S*)-MTPA

**Figure 3**  $\Delta\delta_{S-R}$  values (in ppm) obtained for (*R*)- and (*S*)-MTPA esters **1a** and **1b**.

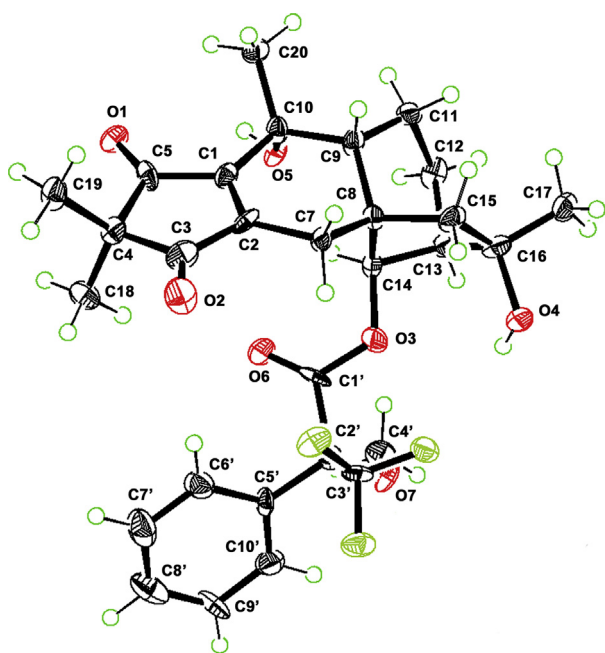


**Figure 4** X-ray structure of **1a**.

1.20, 1.60, and 1.83). The  $^{13}\text{C}$  NMR data ( $\text{C}_5\text{D}_5\text{N}$ , Table 1) reveal 19 carbon resonances that are distinguished *via* DEPT (distortionless enhancement by polarization transfer) and HSQC (heteronuclear single quantum coherence) data to be four methyls, four methylenes, three methines (including one oxygenated at  $\delta_{\text{C}}$  77.0), and eight quaternary carbons (including two carbonyls at  $\delta_{\text{C}}$  207.2 and 206.4, two unsaturated at  $\delta_{\text{C}}$  157.0 and 154.4, and two oxygenated at  $\delta_{\text{C}}$  80.4 and 70.1). The results of above mentioned analysis account for

3 out of 7 degrees of unsaturation, indicating four additional rings in the structure of **1**.

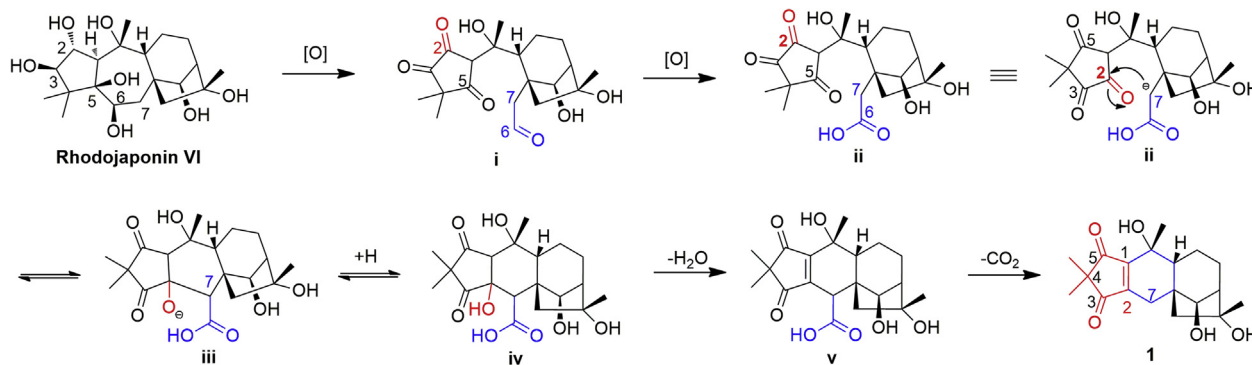
The analysis of the  $^1\text{H}$ – $^1\text{H}$  COSY spectrum of **1**, aided by an HSQC experiment, revealed the connectivity of  $\text{CH}(9)$ – $\text{CH}_2(11)$ – $\text{CH}_2(12)$ – $\text{CH}(13)$ – $\text{CH}(14)$  (fragment a, bolded in Fig. 2). In the HMBC (heteronuclear multiple bond correlation) spectrum of **1** (Fig. 2), correlations from two gem-dimethyl singlets ( $\text{H}_3$ -18 and  $\text{H}_3$ -19) to carbons C-3 ( $\delta_{\text{C}}$  207.2), C-4 ( $\delta_{\text{C}}$  47.8), and C-5 ( $\delta_{\text{C}}$  206.4); from  $\text{H}_2$ -7 to C-1 ( $\delta_{\text{C}}$  157.0), C-2 ( $\delta_{\text{C}}$  154.4), and C-3; and from  $\text{H}_3$ -20 to C-1 allows a 2,2-dimethyl-4-cyclopentene-1,3-dione substructure (ring A in Fig. 1) to be defined. A six-membered ring (ring B in Fig. 1) was determined by the HMBC correlations from  $\text{H}_2$ -7 to C-1, C-2, C-3, C-8, and C-9 as well as the correlations from  $\text{H}_3$ -20 to C-1, C-9, and C-10. In the same way, the structures of rings C and D were established by the HMBC correlations from  $\text{H}_2$ -7 and  $\text{H}_2$ -15 to C-9 and C-14 (two ends of fragment a), which are the same as those of typical grayananes. Thus, the planar structure of **1** was determined to possess an unprecedented 5/6/6/5-fused ring system incorporating a cyclopentene-1,3-dione scaffold.

The relative stereochemistry for **1** was established by analysis of its NOESY (nuclear overhauser effect spectroscopy) spectrum. NOE correlations of H-14/H-12 and H-12/H-13 indicates the chair conformation of ring C, also suggesting the 1,3-diaxial orientation of H-12 and H-14 and the equatorial orientation of H-13. NOE correlation between H-9 and H-15b suggests that H-9 is equatorial because C-15 and C-16 must adopt a 1,3-diaxial orientation to form a bicyclo[3.2.1]octane ring system. In contrast,  $\text{H}_3$ -17 correlates with H-12b, which means that C-17 is in the  $\beta$ -orientation. Therefore, key NOEs of H-14/H-12, H-12/H-13, H-9/ $\text{H}_3$ -20, H-9/H-7b, H-9/H-15b, H-15b/ $\text{H}_3$ -17, and H-12b/ $\text{H}_3$ -17 indicates that H-9,  $\text{CH}_3$ -20, H-7b, H-15b, and  $\text{CH}_3$ -17 are co-facial (Fig. 2). Efforts to determine the absolute configuration of compound **1** using the modified Mosher's method were undertaken<sup>10</sup>. The reaction of **1** with the (*S*)- and (*R*)-MTPA acid chlorides gave the Mosher esters **1a** and **1b**, respectively. 1D and 2D NMR data allow assignment of the proton signals for **1a** and **1b**. Analysis of the  $\Delta\delta_{S-R}$  values for the two diastereomeric esters **1a** and **1b** (Fig. 3) enabled assignment of the absolute configuration at C-14 as *R*. Then, 8*S*, 9*R*, 10*R*, 13*R*, 14*R*, and 16*R* configurations could be assigned to **1** on the basis of relative configuration.

Fortunately, a crystal of **1a** was obtained from MeOH/ $\text{H}_2\text{O}$ . The crystal structure was obtained by X-ray diffraction (Fig. 4) with a Flack parameter of  $-0.2(4)$ . The crystallographic data of **1** have been deposited (deposition number 1885773) at the Cambridge Crystallographic Data Centre (CCDC, Cambridge, UK). The X-ray crystallographic data corroborated the planar structure and provided independent confirmation of the absolute configuration assignment of **1**, obtained by the modified Mosher's method.

Rhomollone A (**1**) is the first example of a rearranged grayanane skeleton with unique 5/6/6/5 tetra-cyclic ring system. We named this new skeleton “rhomollane”. The plausible biosynthetic origin of the rhomollane skeleton could be traced back to a grayanane precursor (rhodojaponin VI) as shown in Scheme 1. In the pathway we proposed, key steps involving oxidation, oxidative ring-opening, and intramolecular aldol condensation lead to the production of intermediate **iv**<sup>11</sup>. Then, intermediate **iv** undergoes dehydration and decarboxylation steps to afford **1**.

Rhomollone XLIII (**2**),  $[\alpha]_{\text{D}}^{20} -11.0$  (*c* 0.1, MeOH), was obtained as a white amorphous powder. The molecular formula of **2** was established to be  $\text{C}_{40}\text{H}_{64}\text{O}_{12}$  by HR-ESIMS data at  $m/z$  735.4313  $[\text{M}-\text{H}]^-$  (Calcd. 735.4325) corresponding to 9



**Scheme 1** Proposed biosynthetic pathway for **1**.

degrees of unsaturation. The  $^1\text{H}$  and  $^{13}\text{C}$  NMR data of **2** (Table 1) provide evidence for half of the expected proton and carbon resonances, which are assigned as belonging to four methyls, four methylenes, seven methines (including four oxygenated at  $\delta_{\text{C}}$  76.1, 81.8, 84.6, and 86.7), and five quaternary carbons (including three oxygenated at  $\delta_{\text{C}}$  77.3, 79.4, and 85.5). The above data are consistent with the feature of typical grayanoids.

Further structure elucidation based on  $^1\text{H}$ - $^1\text{H}$  COSY, HSQC, and HMBC experiments (Fig. 5) reveal a high degree of similarity with those previously reported for rhodojaponin VI<sup>2</sup>. However, a peculiar correlation from the signal at  $\delta_{\text{H}}$  5.57 (H-14) to the signal at  $\delta_{\text{C}}$  84.6 assigned to the carbon C-2 (actually C-2') that was observed in the HMBC spectrum allow us to assume that the compound had a dimeric structure, in which C-14 and C-2' as well as C-2 and C-14' are linked *via* oxygen bridges.

The relative configuration of **2** was assigned mainly using NOESY correlations (Fig. 5). Key NOEs of H-1/H-14, H-1/H-6, H-6/H<sub>3</sub>-18, and H-3/H<sub>3</sub>-18 establish the  $\alpha$ -orientation for H-1, CH<sub>3</sub>-18, H-14, H-6, and H-3. Similarly, the NOE correlations of OH-3/H<sub>3</sub>-19, Hb-11/H<sub>3</sub>-17, H-2/H<sub>3</sub>-20, OH-5/H<sub>3</sub>-19, OH-5/H<sub>3</sub>-20, OH-10/Ha-11, and OH-5/H-9 indicate that OH-3, H-2, CH<sub>3</sub>-19, CH<sub>3</sub>-17, CH<sub>3</sub>-20, OH-5, and H-9 are  $\beta$ -oriented.

Upon treatment of **2** with 1 equiv. of 4-bromobenzoyl chloride in pyridine, a 4-bromobenzoic acid ester **2a** was obtained as the major product. The HR-ESIMS data establish the molecular formula of **2a** as C<sub>47</sub>H<sub>67</sub>BrO<sub>13</sub> ( $m/z$  917.3674 [M-H]<sup>-</sup>, Calcd. 917.3692), which is consistent with the result expected for a monoacylated product. In addition, the signal for H-3 is shifted significantly downfield (from  $\delta_{\text{H}}$  4.07 to 5.46) relative to that of **2**, indicating that the hydroxyl group

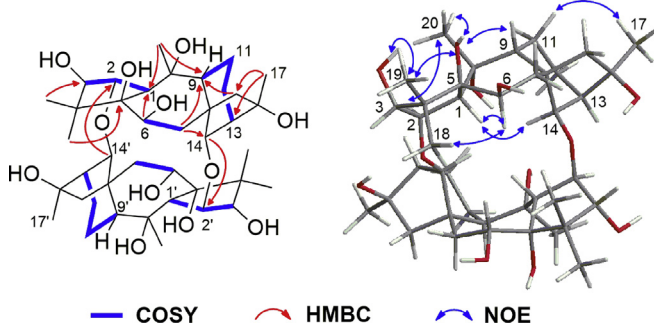


**Figure 5** Selected  $^1\text{H}$ - $^1\text{H}$  COSY, HMBC, and NOE correlations for compound **2**.

at C-3 is acylated in **2a**. HMBC and HSQC data were obtained for **2a** to verify the proposed structure. The HMBC correlations observed from H-3 to ester carbonyl at  $\delta_{\text{C}}$  165.7 confirm the acylation site at C-3. A systematic conformational analysis was performed for **2a-1** (one of the possible enantiomers of **2a**, Fig. 6) using the MMFF94 molecular mechanics force field calculation, which afforded two major conformers (Supporting Information).

The ECD (electronic circular dichroism) calculation was performed after optimization of the selected conformers using the ZINDO method<sup>12</sup>. The experimental ECD spectrum of **2a** agrees well with the calculated ECD of **2a-1** (1*S*,2*R*,3*R*,5*R*,6*R*,8*S*,9*R*,10*R*,13*R*,14*R*,16*R*) and is the opposite of that of **2a-2** (Fig. 6). Thus, the absolute configuration of **2** is established. Rhodomollein XLIII (**2**) is a dimeric grayanoid with a C<sub>2</sub> symmetry axis, containing a novel 14-membered heterocyclic ring.

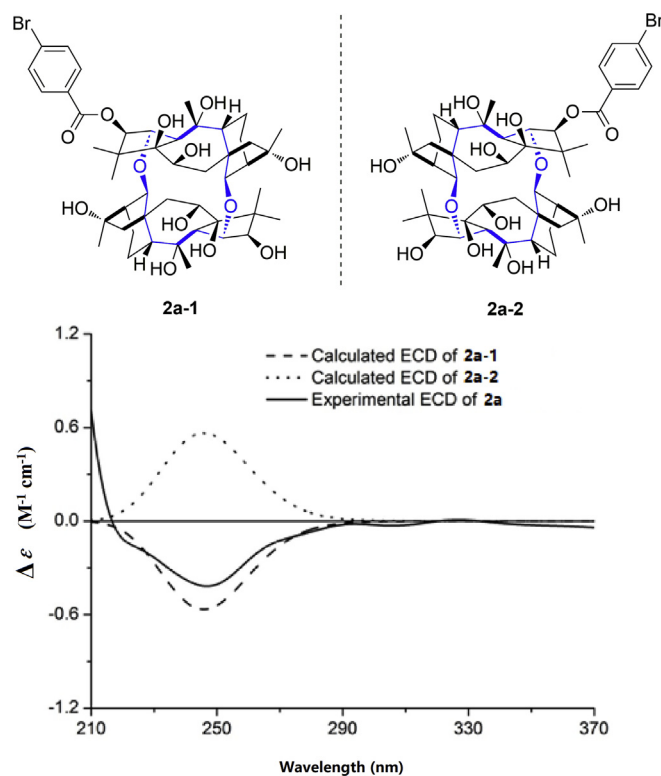


**Figure 6** Calculated and experimental ECD spectra of **2a**.

**Table 2**  $^1\text{H}$  NMR spectroscopic data for compounds **3**–**7** in pyridine- $d_5$  ( $\delta$  in ppm,  $J$  in Hz).

No.	<b>3</b> <sup>b</sup>	<b>4</b> <sup>a</sup>	<b>5</b> <sup>b</sup>	<b>6</b> <sup>a</sup>	<b>7</b> <sup>c</sup>
1	3.72, d (10.8)	3.84, d (9.0)	2.78, d (10.2)	2.17, m	3.01, d (7.2)
2	4.98, m	5.06, dd (9.0, 3.0)	5.15, ddd (10.2, 7.2, 3.6)	4.84, dd (9.0, 3.0)	4.57, dd (8.8, 7.2)
3	4.11, d (4.2)	4.07, d (3.0)	4.00, dd (7.2, 5.4)	4.10, d (3.0)	4.61, d (8.8)
4	—	—	—	—	—
5	—	—	—	—	—
6	4.50, brd (6.6)	5.79, brd (4.5)	5.01, m	4.35, brd (10.5)	4.29, brd (4.8)
7	2.83, d (12.0) 2.98, m	2.81, dd (16.0, 5.5) 2.90, brd (16.0)	2.50, dd (13.2, 10.8) 3.00, dd (13.2, 4.8)	2.73, brd (14.0) 3.05, dd (14.0, 10.5)	1.88, dd (14.4, 4.8) 2.78, brd (14.4)
8	—	—	—	—	—
9	—	—	2.14, m	—	2.12, dd (9.6, 7.2)
10	—	—	—	3.33, m	—
11	2.37, m 2.72, dd (14.4, 6.6)	2.20, m 2.63, m	1.62, m 2.17, m	5.29, brs	1.48, m 1.62, m
12	1.49, m 1.73, m	1.46, m 1.76, m	1.73, m 2.71, m	2.25, m 2.34, m	1.68, m 1.74, m
13	2.42, brs	2.42, m	2.54, brs	2.55, brd (3.5)	2.26, brd (7.2)
14	4.09, d (6.0)	4.03, brs	5.11, brd (7.2)	4.56, brs	4.96, brs
15	2.45, d (15.6) 2.94, d (15.6)	2.39, d (15.0) 2.73, d (15.0)	2.18, d (14.4) 2.33, d (14.4)	2.16, d (13.5) 2.29, d (13.5)	1.95, d (14.0) 2.34, d (14.0)
16	—	—	—	—	—
17	1.45, s	1.62, s	1.56, s	1.49, s	1.49, s
18	1.07, s	1.21, s	4.11, dd (10.8, 5.4) 4.25, dd (10.8, 3.6)	1.45, s	1.51, s
19	1.38, s	1.48, s	1.79, s	1.81, s	1.48, s
20	2.32, s	2.14, s	1.96, s	1.65, d (7.0)	1.58, s
1'	5.88, s	—	—	—	—
2'	—	1.94, s	—	—	—
3'	7.65, brs	—	—	—	—
4'	—	—	—	—	—
5'	—	—	—	—	—
6'	7.33, brd (8.0)	—	—	—	—
7'	7.25, brd (8.0)	—	—	—	—

<sup>a</sup>Recorded at 500 MHz. <sup>b</sup>Recorded at 600 MHz. <sup>c</sup>Recorded at 800 MHz. —Not applicable.

Compound **3** (rhodomollein XLIV) was obtained as an amorphous solid and had the molecular formula  $\text{C}_{27}\text{H}_{36}\text{O}_8$  based on the HR-ESIMS data, acquiring an index of hydrogen deficiency (IHD) of 10. The  $^1\text{H}$ ,  $^{13}\text{C}$ , and DEPT NMR spectroscopic data of **3** (Tables 2 and 4) display signals assignable to a grayanane attached with a 1,3,5-trisubstituted aromatic moiety [ $\delta_{\text{H}}$  7.65 (brs), 7.33 (brd,  $J = 8.0$  Hz), and 7.25 (brd,  $J = 8.0$  Hz)]. The  $^1\text{H}$  and  $^{13}\text{C}$  NMR data of **3** are similar to those of a known diterpenoid, rhodomicanol B<sup>13</sup>. The only difference is that **3** is found to have an additional hydroxyl group and the double bond is at different position. The HMBC correlations from H-2 to C-1, C-3, C-4, and C-5 place the additional hydroxyl at C-2. Meanwhile, the double bond was determined to be at  $\Delta^{9(10)}$  by HMBC correlations from H-2 to C-10, H<sub>2</sub>-7 to C-9, as well as H<sub>3</sub>-20 to C-9 and C-10. The key NOESY correlation between H-1' and H-6 suggested that H-1' is also  $\alpha$ -oriented<sup>13</sup>.

Compound **4** (rhodomollein XLV) was obtained as a white powder with the molecular formula of  $\text{C}_{22}\text{H}_{34}\text{O}_7$  on the basis of (+)-HR-ESIMS ion peak at  $m/z$  433.2202 [ $\text{M}+\text{Na}$ ]<sup>+</sup> (Calcd. for  $\text{C}_{22}\text{H}_{34}\text{O}_7\text{Na}$ , 433.2197) and  $^{13}\text{C}$  NMR data (Table 4), suggesting that **4** possessed 6 degrees of unsaturation. A comparison of its  $^1\text{H}$  and  $^{13}\text{C}$  NMR spectra with those of rhodomollein XXVI reveals the two structures to be closely related<sup>2</sup>. The only difference is the presence of signals at  $\delta_{\text{H}}$  170.8, 21.8 and  $\delta_{\text{C}}$  1.94 corresponding to an additional acetyl group in **4**. In the HMBC spectrum, cross-peaks due to the signals for H-6 ( $\delta_{\text{H}}$  5.79) with the carbon signals at  $\delta_{\text{C}}$  170.8 (C-1') were observed, and

consequently it was inferred that the acetyl group is attached at C-6.

The HR-ESIMS of compound **5** (rhodomollein XLVI) gives a molecular formula of  $\text{C}_{20}\text{H}_{34}\text{O}_8$ . The  $^1\text{H}$  and  $^{13}\text{C}$  NMR data of **5** closely resemble those for rhodojaponin VI<sup>2</sup>. The major difference between the two compounds is that a methyl of **5** is substituted by a hydroxyl group. The hydroxyl is placed at C-18 by the HMBC correlations from H<sub>2</sub>-18 to C-3, C-4, C-5, and C-19.

The molecular formula of compound **6** (rhodomollein XLVII) was deduced as  $\text{C}_{20}\text{H}_{32}\text{O}_6$  by HR-ESIMS with an IHD of 5. Analysis of the NMR spectra shows that compound **6** has a typical grayanane skeleton with one double bond ( $\delta_{\text{H}}$  5.29;  $\delta_{\text{C}}$  113.8 and 157.2). The double bond was determined to be at  $\Delta^{9(11)}$  by HMBC correlations from proton at  $\delta_{\text{H}}$  5.29 to C-8, C-9, C-10, and C-13. A group of methyl protons appears as a doublet and correlated with C-1, C-9, and C-10 in the HMBC spectrum, suggesting that the C-10 position is unhydroxylated. Key NOESY correlations of H-10/H-7b and H-15b/H-7a indicate the  $\alpha$ -configuration for H-7b and H-10.

Compound **7** (rhodomollein XLVIII) exhibits a molecular formula of  $\text{C}_{20}\text{H}_{32}\text{O}_6$ , as deduced from its HR-ESIMS data, which indicate an IHD of 5. Its NMR spectroscopic data are comparable to those of principinol B with exception of absence of the double bond and the C-2 and C-16 of compound **7** are hydroxylated. In the NOESY spectrum, key correlations of H-2/H<sub>3</sub>-19, H-3/H<sub>3</sub>-18, H-1/H-3, H-1/H-14, H-6/H<sub>3</sub>-19, H-9/H-15a, and H-15a/H<sub>3</sub>-17 suggest a  $\beta$ -configuration for H-2 and H<sub>3</sub>-17.

**Table 3**  $^1\text{H}$  NMR spectroscopic data for compounds **8–12** in pyridine- $d_5$  ( $\delta$  in ppm,  $J$  in Hz).

No.	<b>8</b> <sup>a</sup>	<b>9</b> <sup>a</sup>	<b>10</b> <sup>a</sup>	<b>11</b> <sup>a</sup>	<b>12</b> <sup>a</sup>
1	3.27, d (4.0)	3.02, d (7.5)	5.28, dd (9.0, 5.0)	2.68, m	2.44, dt (13.0, 3.5)
2	6.19, brd (4.0)	5.13, m	2.42, m	2.30, m	1.53, m
			2.73, m	2.67, m	2.38, t (13.0)
3	3.99, brd (4.5)	3.98, brs	—	4.20, brs	3.50, brd (8.0)
4	—	—	—	—	—
5	—	—	4.26, brs	—	3.95, brd (2.5)
6	4.72, brs	5.83, dd (11.5, 4.5)	4.97, m	2.81, dt (12.0, 3.0)	1.97, m
7	2.61, m	2.40, dd (13.5, 11.5)	2.51, m	1.82, m	1.92, m
	2.96, dd (13.5, 4.0)	2.69, dd (13.5, 4.5)	—	2.22, m	2.58, m
8	—	—	—	—	—
9	2.19, brd (6.5)	2.18, m	2.24, m	1.69, m	1.81, m
10	—	—	—	—	—
11	1.69, m	1.74, m	1.96, m	1.89, m	1.97, m
	2.01, dd (14.5, 6.5)	2.17, m	—	2.57, dd (15.0, 7.0)	2.62, m
12	1.64, m	1.55, m	4.07, m	2.04, m	2.05, m
	2.61, m	2.53, m	—	2.14, dd (13.0, 7.0)	2.18, m
13	2.50, brs	2.84, brs	3.13, m	—	—
14	5.07, brd (7.0)	5.15, m	3.14, m	2.05, m	2.12, d (10.5)
				2.22, m	2.29, d (10.5)
15	2.15, d (14.5)	5.11, s	1.89, d (13.0)	1.71, m	1.81, m
	2.31, d (14.5)	—	1.98, d (13.0)	2.19, d (14.0)	2.21, d (14.0)
16	—	—	—	—	—
17	1.54, s	1.77, s	1.84, s	1.45, s	1.49, s
18	1.48, s	1.38, s	1.74, s	1.21, s	1.51, s
19	1.74, s	1.58, s	1.57, s	1.50, s	0.94, s
20	1.90, s	1.94, s	1.69, s	1.61, s	1.53, s
1'	—	—	—	—	—
2'	2.63, m	1.98, s	—	—	—
	2.66, m	—	—	—	—
3'	2.60, m	—	—	—	—
	2.70, m	—	—	—	—
4'	—	—	—	—	—
5'	3.59, s	—	—	—	—

<sup>a</sup>Recorded at 500 MHz. —Not applicable.

Compound **8** (rhodomollein XLIX) gives a molecular ion peak at  $m/z$  523.2517  $[\text{M}+\text{Na}]^+$  in the HR-ESIMS (Calcd. 523.2514), corresponding to the molecular formula  $\text{C}_{25}\text{H}_{40}\text{O}_{10}$  (6 IHD). A comparison of the NMR data of **8** with those of rhodojaponin VI indicates that the two compounds have the same structures, except for the mono-methyl succinate group<sup>2</sup>. The mono-methyl succinate group is located at C-2 based on the HMBC correlations from H-2 to  $\delta_{\text{C}}$  172.6 (C-1').

The molecular formula of **9** (rhodomollein L) was determined as  $\text{C}_{22}\text{H}_{34}\text{O}_7$  by HR-ESIMS. The  $^1\text{H}$  and  $^{13}\text{C}$  NMR data of **9** are similar to those of rhodomollein X<sup>14</sup>. However, signals for an additional acetyl group ( $\delta_{\text{C}}$  21.9 and 170.2) in **9** were observed. In the HMBC spectrum, the H-6 proton shows a  $^3J$  correlation with the carbonyl carbon of the acetyl group ( $\delta_{\text{C}}$  170.2), confirming the location of the acetyl group at C-6.

Compound **10** (rhodomollein LI) was determined to have the molecular formula  $\text{C}_{20}\text{H}_{32}\text{O}_6$ , from the HR-ESIMS ( $m/z$  391.2106  $[\text{M}+\text{Na}]^+$ , Calcd. 391.2091) and NMR spectra, implying 5 IHD. The NMR data of **10** are similar to those of seco-rhodomollone with two exceptions<sup>15</sup>. First, the carbonyl group in **10** is located at C-3 instead of C-5, which is supported by the HMBC correlations from H-1 and H<sub>2</sub>-2 to C-3 ( $\delta_{\text{C}}$  215.2). Second, compound **10** has an additional hydroxyl group at C-12, and this assignment is supported by the HMBC correlations from H-9, H-13, and H-14 to C-12 ( $\delta_{\text{C}}$  75.6). The NOE correlations of H-12/H<sub>3</sub>-17 and H-12/H-9 indicate that the OH-12 is  $\alpha$ -oriented.

The molecular formula of **11** (rhodomollein LII) is defined as  $\text{C}_{20}\text{H}_{32}\text{O}_5$ , indicating an IHD of five. The NMR data of **11** are similar to those of rhododecorumin III<sup>16</sup>. Further structural analysis *via* 2D NMR data indicates that **11** has a 10-OH group instead of the terminal double bond at  $\Delta^{10(20)}$ . The NOE correlations of H-1/H-9, HO-3/H-1, H-6/H<sub>3</sub>-18, and H-6/H<sub>3</sub>-20 indicate that HO-3, H-1, and H-9 are  $\beta$ -oriented and that H-6, CH<sub>3</sub>-18, and CH<sub>3</sub>-20 are  $\alpha$ -oriented.

Compound **12** (rhodomollein LIII) was obtained as white powder. The molecular formula, deduced to be  $\text{C}_{20}\text{H}_{34}\text{O}_5$  by HR-ESIMS, contains two more protons than **11**. The  $^1\text{H}$  and  $^{13}\text{C}$  NMR spectra of compound **12** show distinct similarities with compound **11** except that the carbonyl group at C-5 is reduced to hydroxyl group in **12**, which is proved by the HMBC correlations from H-1, H-7, H<sub>3</sub>-18, and H<sub>3</sub>-19 to C-5 ( $\delta_{\text{C}}$  77.0). In the NOESY spectrum of **12**, the correlations of OH-5/H-1, OH-3/H-1, H-1/H-9, and H-6/H<sub>3</sub>-20 suggest that OH-3, OH-5, H-1, and H-9 are  $\beta$ -oriented and that H-6 and CH<sub>3</sub>-20 are  $\alpha$ -oriented.

The other known compounds isolated were identified as 2-*O*-methylrhodojaponin VI (**13**)<sup>17</sup>, 2-*O*-methylrhodomollein XI (**14**)<sup>17</sup>, rhodomollein XI (**15**)<sup>14</sup>, *seco*-rhodomollone (**16**)<sup>15</sup>, and kalmanol (**17**)<sup>18</sup> by comparison of experimental and reported spectroscopic data.

The antinociceptive activities of compounds **3**, **4**, **6**, **7**, and **12–17** were evaluated by an acetic acid-induced writhing test, as

**Table 4**  $^{13}\text{C}$  NMR spectroscopic data for compounds **3–12** in pyridine- $d_5$  ( $\delta$  in ppm).

No.	<b>3</b> <sup>b</sup>	<b>4</b> <sup>a</sup>	<b>5</b> <sup>b</sup>	<b>6</b> <sup>a</sup>	<b>7</b> <sup>c</sup>	<b>8</b> <sup>a</sup>	<b>9</b> <sup>a</sup>	<b>10</b> <sup>a</sup>	<b>11</b> <sup>a</sup>	<b>12</b> <sup>a</sup>
1	50.2	52.9	54.8	57.8	59.7	60.3	59.1	122.8	50.3	42.0
2	82.0	82.2	78.4	83.8	77.8	84.7	80.1	34.2	29.2	44.6
3	88.1	88.2	81.5	90.4	84.1	85.6	86.6	215.2	78.0	80.5
4	46.3	47.9	53.9	48.2	46.9	51.1	49.7	52.2	50.6	38.8
5	93.6	84.9	82.2	85.4	89.0	85.9	83.5	78.4	216.1	77.0
6	77.1	71.6	74.4	72.4	76.9	74.6	78.2	71.6	45.6	37.4
7	38.8	39.4	44.9	35.7	32.6	44.9	37.2	39.9	41.0	29.8
8	57.2	57.2	52.6	52.5	47.1	52.9	55.8	84.9	41.1	41.7
9	138.1	138.7	56.1	157.2	57.5	55.5	49.4	50.0	54.6	55.2
10	124.9	124.2	78.5	31.3	83.7	77.9	79.3	140.4	75.0	75.1
11	26.8	26.5	22.5	113.8	19.4	22.9	23.1	42.1	20.8	21.0
12	27.1	27.0	27.7	30.7	25.2	27.3	25.1	75.6	34.6	34.7
13	54.6	54.2	57.1	55.0	52.9	57.0	56.8	65.1	81.0	81.1
14	88.6	88.6	79.8	80.8	79.2	79.7	79.8	55.9	43.7	43.9
15	60.6	59.3	60.8	59.3	62.1	60.9	132.0	52.4	56.6	56.8
16	82.6	82.6	80.3	81.6	79.8	80.2	138.5	80.8	76.6	76.7
17	24.5	24.6	24.5	27.6	25.3	24.4	16.0	24.2	22.2	22.3
18	27.1	25.9	68.7	26.3	23.9	23.1	25.5	24.3	25.7	25.9
19	18.6	18.6	16.8	21.5	17.5	20.8	21.1	22.5	22.8	25.3
20	19.3	19.3	30.3	18.8	23.0	29.6	29.9	12.2	21.3	21.9
1'	104.9	170.8	—	—	—	172.6	170.2	—	—	—
2'	131.0	21.8	—	—	—	30.4	21.9	—	—	—
3'	117.4	—	—	—	—	29.8	—	—	—	—
4'	147.8	—	—	—	—	173.2	—	—	—	—
5'	149.0	—	—	—	—	52.0	—	—	—	—
6'	116.4	—	—	—	—	—	—	—	—	—
7'	120.7	—	—	—	—	—	—	—	—	—

<sup>a</sup>Recorded at 125 MHz. <sup>b</sup>Recorded at 150 MHz. <sup>c</sup>Recorded at 200 MHz. —Not applicable.

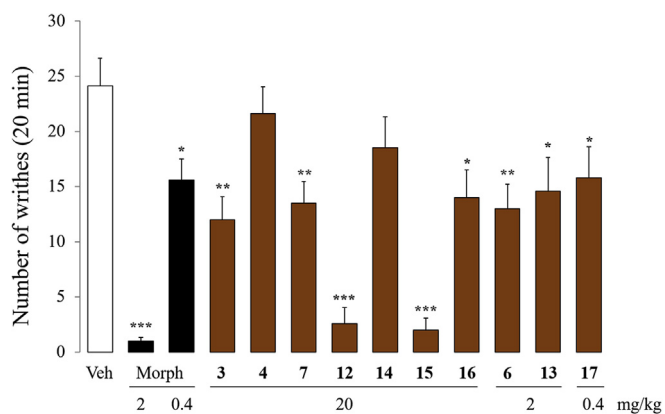


**Figure 7** Antinociceptive activities of the compounds (acetic acid-induced writhing test). Morphine (morph) was used as the control. Each bar and vertical line represent the mean  $\pm$  SEM of the values obtained from 8 mice. \* $P < 0.05$ , \*\* $P < 0.01$ , \*\*\* $P < 0.001$ , represent statistically significant differences between the test compound groups or the control groups and the vehicle group (veh) (one-way ANOVA followed by the Bonferroni test).

described earlier<sup>2</sup>. Compounds **1** and **2** were not tested due to the lack of quantities after completing the structural determination. As shown in Fig. 7, compounds **3**, **7**, **12**, **15** and **16** displayed significant antinociceptive activities at a dose of 20 mg/kg with inhibition rates ranging from 41.9% to 91.6% [inhibition rates: (average number of writhes in the vehicle group—average number of writhes in the experimental group)/average number of writhes in the vehicle

group]. Among them, compounds **12** and **15** exhibited the highest potency with inhibition rates of 89.0% and 91.6%, respectively. Compounds **6** and **13** inhibited 46.0% and 39.4% of the acetic acid-induced writhes at a dose of 2 mg/kg, while compound **17**, with a kalmane skeleton, was found to be active at a dose of 0.4 mg/kg (with inhibition rate of 34.3%). Compound **13**, without an acetyl group at C-6, showed higher antinociceptive activity, compared with compound **14** with an acetyl group at C-6, which were inactive. This finding suggests that the acetyl group at C-6 might hamper the antinociceptive activity of grayanane-derived diterpenoids. In addition, compound **14**, in which OH-2 was methylated, was less potent than **15**. This result suggests that methylation at OH-2 might reduce the antinociceptive activity.

### 3. Conclusions

The present investigation of the flowers of *R. molle* has yielded 17 diterpenoids including 12 new compounds (**1–12**). Among them, rhomollone A (**1**) possesses an unprecedented 5/6/6/5 tetra-cyclic ring system (B-nor grayanane) incorporating a cyclopentene-1,3-dione scaffold while rhodomollein XLIII (**2**) is a dimeric grayanoid, containing a novel 14-membered heterocyclic ring with a  $C_2$  symmetry axis. Compounds **3**, **7**, **12**, **15** and **16** showed significant antinociceptive activities at a dose of 20 mg/kg with inhibition rates ranging from 41.9% to 91.6%. Compounds **6** and **13** inhibited 46.0% and 39.4% of the acetic acid-induced writhes at a dose of 2 mg/kg, while compound **17** inhibited 34.3% of the writhes at a dose of 0.4 mg/kg. These results support the use of this plant in traditional Chinese medicine for migraine headache, and other pain symptoms.

## 4. Experimental

### 4.1. General experimental procedures

Optical rotations were measured on a PE model 343 polarimeter (PerkinElmer, Waltham, MA, USA). CD spectra were recorded on a JASCO-815 CD spectrometer (JASCO, Tokyo, Japan). IR spectra were recorded on a Nicolet 5700 FT-IR microscope instrument (Thermo Fisher Scientific, Waltham, MA, USA). NMR spectra were obtained on INOVA-500 (Varian, Palo Alto, CA, USA) and Bruker AV600-III (Bruker, Billerica, MA, USA) spectrometers, in  $C_5D_5N$  with solvent peaks used as references. ESIMS were measured on an Agilent 1100 Series LC/MSD Trap mass spectrometer (Agilent, Santa Clara, CA, USA). HR-ESIMS data were measured using an Agilent 6520 Accurate-Mass Q-TOF LC/MS spectrometer (Agilent). Preparative HPLC was performed on a Shimadzu LC-6AD instrument with SPD-20A and RID-10A detectors (Shimadzu, Kyoto, Japan) using an YMC Pack ODS-A column (250 mm  $\times$  20 mm, 5  $\mu$ m, YMC, Kyoto, Japan). Macroporous resin (D101 type, the Chemical Plant of NanKai University, Tianjin, China), Si gel (160–200 and 200–300 mesh, Qingdao Marine Chemical Factory, China) was used for column chromatography (CC). TLC was carried out with glass precoated Si gel GF<sub>254</sub> plates (Qingdao Marine Chemical Factory). Spots were visualized under UV light or by spraying with 10%  $H_2SO_4$  in EtOH/ $H_2O$  (95:5, *v/v*) followed by heating.

### 4.2. Animals

All animal care and experimental procedures were in accordance with the current guidelines of the National Institutes of Health (NIH, USA). Animal experiments were approved by the Ethics Committee of Institute of Materia Medica, Chinese Academy of Medical Sciences and Peking Union Medical College (Beijing, China). All experiments were carried out with both male and female Kunming mice (Institute of Laboratory Animal Sciences, Chinese Academy of Medical Sciences and Peking Union Medical College, Beijing, China) weighing 18–22 g each (approximately 6 weeks old). The animals were housed for at least 3 days (before use) at a temperature of  $22 \pm 1$  °C, under a 12 h cycle of light-dark, with free access to food and water. The dose for each trial was determined from the preliminary experiments. To minimize the subjective bias, the behavioral responses in each experiment were recorded by three independent observers. The observers who performed the behavioral experiment were blind to the group of the animals.

### 4.3. Plant material

Flowers of *R. molle* were collected in Xingan, Guangxi province, China, in November 2012 and positively identified by Prof. Songji Wei of Guangxi Traditional Medical College. A voucher specimen (ID-s-2446) was preserved in the herbarium at the Department of Medicinal Plants, Institute of Materia Medica, Chinese Academy of Medical Sciences (Beijing, China).

### 4.4. Extraction and isolation

The air-dried flowers of *R. molle* (74 kg) were extracted by EtOH (95:5, *v/v*) at reflux for three times (2 h each time). The crude extract (not completely dried, 9.85 kg) was extracted successively with petroleum ether,  $CH_2Cl_2$ , EtOAc, and MeOH on a Soxhlet extractor. The EtOAc extract (650 g) was separated on a

macroporous resin column and eluted sequentially with 70:30, 55:45, 40:60, and 5:95 (*v/v*)  $H_2O$ /EtOH solutions. The 30% EtOH fraction (150.9 g) was further separated on an MCI gel column and eluted in a gradient of MeOH/ $H_2O$  (1:9–10:0, *v/v*) to obtain 13 fractions ( $F_1$ – $F_{13}$ ). Fraction  $F_{11}$  (11 g) was further separated on a Sephadex LH-20 column eluted with MeOH/ $H_2O$  (60:40, *v/v*) to yield 11 fractions ( $F_{11}S_1$ – $F_{11}S_{11}$ ). Fraction  $F_{11}S_3$  (2.6 g) was separated with ODS column and eluted with MeOH/ $H_2O$  (1:9–10:0, *v/v*) to yield 10 fractions ( $F_{11}S_3P_1$ – $F_{11}S_3P_{10}$ ). Fraction  $F_{11}S_3P_6$  was further purified by semi-preparative HPLC with MeOH/ $H_2O$  (48:52, *v/v*, 3.5 mL/min) to yield compound **1** (8.7 mg). Fraction  $F_{11}S_3P_8$  was further purified by semi-preparative HPLC with MeOH/ $H_2O$  (58:42, *v/v*, 3.5 mL/min) to yield compound **16** (33.4 mg). Fraction  $F_{11}S_4$  (0.7 g) was separated with semi-preparative HPLC with ACN/ $H_2O$  (25:75, *v/v*, 3.5 mL/min) to yield compounds **10** (3.8 mg) and **15** (168.4 mg). Fraction  $F_{10}$  (29 g) was further separated on a Sephadex LH-20 column eluted with MeOH/ $H_2O$  (60:40, *v/v*) to yield 5 fractions ( $F_{10}S_1$ – $F_{10}S_5$ ). Fraction  $F_{10}S_3$  (3.1 g) was separated with ODS column and eluted with MeOH/ $H_2O$  (1:9–10:0, *v/v*) to yield 8 fractions ( $F_{10}S_3P_1$ – $F_{10}S_3P_8$ ). Fraction  $F_{10}S_3P_6$  was further purified by semi-preparative HPLC with MeOH/ $H_2O$  (45:55, *v/v*, 3.5 mL/min) to yield compounds **8** (3.9 mg), **13** (27.0 mg), and **17** (34.3 mg). Fraction  $F_{10}S_3P_5$  was further purified by semi-preparative HPLC with MeOH/ $H_2O$  (45:55, *v/v*, 3.5 mL/min) to yield compounds **4** (8.9 mg) and **7** (27.1 mg). Fraction  $F_{10}S_3P_7$  was further purified by semi-preparative HPLC with ACN/ $H_2O$  (22:78, *v/v*, 6 mL/min) to yield compound **11** (3.0 mg), **12** (18.2 mg), and **14** (84.6 mg). Fraction  $F_{10}S_3P_8$  was further purified by semi-preparative HPLC with ACN/ $H_2O$  (25:75, *v/v*, 3.5 mL/min) to yield compounds **2** (9.3 mg), **3** (62.7 mg), **5** (1.6 mg), **6** (13.6 mg), and **9** (25.0 mg).

#### 4.4.1. Preparation of (R)-MTPA ester **1a**

To a solution of **1** (2 mg, 0.006 mmol) in anhydrous pyridine (1 mL) was added (S)-MTPACl (1.5 mg, 0.006 mmol). After stirring at room temperature for 4 h, water was added. The reaction mixture was evaporated to dryness, and subjected to semi-preparative HPLC using ACN in  $H_2O$  (60:40) as the mobile phase to give **1a** (0.9 mg). Compound **1a**: HR-ESIMS *m/z*: 549.2111 [M–H]<sup>–</sup> (Calcd. 549.2106 for  $C_{29}H_{32}O_7F_3$ ).

#### 4.4.2. Preparation of (S)-MTPA ester **1a**

To a solution of **1** (2 mg, 0.006 mmol) in anhydrous pyridine (1 mL) was added (R)-MTPACl (1.5 mg, 0.006 mmol). After stirring at room temperature for 4 h, water was added. The reaction mixture was evaporated to dryness, and subjected to semi-preparative HPLC using ACN in  $H_2O$  (60:40) as the mobile phase to give **1b** (0.6 mg). Compound **1b**: HR-ESIMS *m/z*: 549.2110 [M–H]<sup>–</sup> (Calcd. 549.2106 for  $C_{29}H_{32}O_7F_3$ ).

#### 4.4.3. Preparation of 2-O-(4-bromobenzoyl)-rhodomollein XLIII (**2a**)

Compound **2** (4 mg, 0.0054 mmol) was transferred into a dry flask; 4-bromobenzoyl chloride (1.2 mg, 0.0054 mmol) was added into the flask, to which was immediately added 1 mL of anhydrous pyridine. The solution was stirred at room temperature for 4 h. After the reaction, water was added. The majority of solvent was evaporated and some MeOH was added to this solution. The solution was separated by reversed-phase preparative HPLC using ACN in  $H_2O$  (40:60) as the mobile phase to give **2a** (1.1 mg). 2-O-



(4-bromobenzoyl)-rhodomollein XLIII (**2a**). HR-ESIMS  $m/z$ : 917.3674  $[M-H]^-$  (Calcd. 917.3692 for  $C_{47}H_{66}BrO_{13}$ ).

#### 4.4.4. Rhomollone A (**1**)

White powder;  $[\alpha]_D^{20}$   $-5.0$  ( $c$  0.1, MeOH); IR  $\nu_{max}$  3256, 2964, 1737, 1689, 1462, 1444, 1377, 1302, 1113, 1045, 945, 926, 884  $cm^{-1}$ ;  $^1H$  and  $^{13}C$  NMR data, [Table 1](#); HR-ESIMS  $m/z$  357.1676  $[M+Na]^+$  (Calcd. for  $C_{19}H_{26}NaO_5$ , 357.1672).

#### 4.4.5. Rhodomollein XLIII (**2**)

White powder;  $[\alpha]_D^{20}$   $-11.0$  ( $c$  0.1, MeOH); IR  $\nu_{max}$  3421, 2952, 2920, 1475, 1445, 1412, 1380, 1162, 1129, 1100, 1045, 963, 879, 789  $cm^{-1}$ ;  $^1H$  and  $^{13}C$  NMR data, [Table 1](#); HR-ESIMS  $m/z$  735.4313  $[M+H]^+$  (Calcd. for  $C_{40}H_{63}O_{12}$ , 735.4325).

#### 4.4.6. Rhodomollein XLIV (**3**)

White powder;  $[\alpha]_D^{20}$   $+45.0$  ( $c$  0.02, MeOH); IR  $\nu_{max}$  3364, 2940, 1614, 1523, 1459, 1414, 1373, 1289, 1084, 1054, 990, 947, 873  $cm^{-1}$ ;  $^1H$  and  $^{13}C$  NMR data, [Tables 2 and 4](#); HR-ESIMS  $m/z$  489.2485  $[M+H]^+$  (Calcd. for  $C_{27}H_{37}O_8$ , 489.2483).

#### 4.4.7. Rhodomollein XLV (**4**)

White powder;  $[\alpha]_D^{20}$   $+32.4$  ( $c$  0.7, MeOH); IR  $\nu_{max}$  3378, 2936, 1719, 1446, 1374, 1255, 1052, 943, 881, 826, 805, 798, 586  $cm^{-1}$ ;  $^1H$  and  $^{13}C$  NMR data, [Tables 2 and 4](#); HR-ESIMS  $m/z$  433.2202  $[M+Na]^+$  (Calcd. for  $C_{22}H_{34}NaO_7$ , 433.2197).

#### 4.4.8. Rhodomollein XLVI (**5**)

White powder;  $[\alpha]_D^{20}$   $-18.1$  ( $c$  0.16, MeOH); IR  $\nu_{max}$  3412, 3297, 2975, 2939, 2916, 1470, 1430, 1406, 1153, 1136, 1097, 1038, 987, 945, 917, 872, 803  $cm^{-1}$ ;  $^1H$  and  $^{13}C$  NMR data, [Tables 2 and 4](#); HR-ESIMS  $m/z$  425.2147  $[M+Na]^+$  (Calcd. for  $C_{20}H_{34}NaO_8$ , 425.2146).

#### 4.4.9. Rhodomollein XLVII (**6**)

White powder;  $[\alpha]_D^{20}$   $-3.3$  ( $c$  0.03, MeOH); IR  $\nu_{max}$  3375, 2937, 1674, 1640, 1456, 1380, 1185, 1139, 1050, 993, 958, 938, 884  $cm^{-1}$ ;  $^1H$  and  $^{13}C$  NMR data, see [Tables 2 and 4](#); HR-ESIMS  $m/z$  391.2093  $[M+Na]^+$  (Calcd. for  $C_{20}H_{32}NaO_6$ , 391.2091).

#### 4.4.10. Rhodomollein XLVIII (**7**)

White powder;  $[\alpha]_D^{20}$   $-16.4$  ( $c$  0.5, MeOH); IR  $\nu_{max}$  3369, 2970, 2956, 2925, 1470, 1446, 1378, 1241, 1129, 1088, 1029, 998, 981, 822, 650, 615, 563  $cm^{-1}$ ;  $^1H$  and  $^{13}C$  NMR data, [Tables 2 and 4](#); HR-ESIMS  $m/z$  391.2093  $[M+Na]^+$  (Calcd. for  $C_{20}H_{32}NaO_6$ , 391.2091).

#### 4.4.11. Rhodomollein XLIX (**8**)

White powder;  $[\alpha]_D^{20}$   $-34.0$  ( $c$  0.7, MeOH); IR  $\nu_{max}$  3378, 2957, 1725, 1442, 1375, 1281, 1219, 1167, 1049, 1000, 879, 848, 798, 706  $cm^{-1}$ ;  $^1H$  and  $^{13}C$  NMR data, [Tables 3 and 4](#); HR-ESIMS  $m/z$  523.2517  $[M+Na]^+$  (Calcd. for  $C_{25}H_{40}NaO_{10}$ , 523.2514).

#### 4.4.12. Rhodomollein L (**9**)

White powder;  $[\alpha]_D^{20}$   $+11.3$  ( $c$  0.4, MeOH); IR  $\nu_{max}$  3384, 2959, 2927, 1716, 1656, 1440, 1376, 1264, 1137, 1079, 1049, 1031, 999, 976, 938, 861, 798, 609  $cm^{-1}$ ;  $^1H$  and  $^{13}C$  NMR data, [Tables 3 and 4](#); HR-ESIMS  $m/z$  433.2197  $[M+Na]^+$  (Calcd. for  $C_{22}H_{34}NaO_7$ , 433.2197).

#### 4.4.13. Rhodomollein LI (**10**)

White powder;  $[\alpha]_D^{20}$   $+10.0$  ( $c$  0.02, MeOH); IR  $\nu_{max}$  3352, 2937, 1696, 1564, 1432, 1369, 1108, 1055, 930, 901, 875, 844  $cm^{-1}$ ;  $^1H$  and  $^{13}C$  NMR data, [Tables 3 and 4](#); HR-ESIMS  $m/z$  391.2106  $[M+Na]^+$  (Calcd. for  $C_{20}H_{32}NaO_6$ , 391.2091).

#### 4.4.14. Rhodomollein LII (**11**)

White powder;  $[\alpha]_D^{20}$   $-12.0$  ( $c$  0.1, MeOH); IR  $\nu_{max}$  3358, 2989, 2942, 2879, 1706, 1445, 1377, 1252, 1164, 1154, 1094, 1071, 1033, 978, 963, 926, 852  $cm^{-1}$ ;  $^1H$  and  $^{13}C$  NMR data, [Tables 3 and 4](#); HR-ESIMS  $m/z$  375.2142  $[M+Na]^+$  (Calcd. for  $C_{20}H_{32}NaO_5$ , 375.2142).

#### 4.4.15. Rhodomollein LIII (**12**)

White powder;  $[\alpha]_D^{20}$   $+19.0$  ( $c$  0.1, MeOH); IR  $\nu_{max}$  3373, 3317, 2937, 2909, 2882, 1473, 1450, 1372, 1345, 1262, 1164, 1095, 1057, 1044, 959, 917, 890, 851  $cm^{-1}$ ;  $^1H$  and  $^{13}C$  NMR data, [Tables 3 and 4](#); HR-ESIMS  $m/z$  377.2296  $[M+Na]^+$  (Calcd. for  $C_{20}H_{34}NaO_5$ , 377.2298).

### 4.5. Acetic acid-induced writhing test

Control groups and test groups were set up, each group consisted of 8 mice. Twenty minutes after administration (the control group received 0.9% NaCl, 5 mL/kg, i.p.), mice were injected with 0.8%  $v/v$  acetic acid solution (injection volume: 0.1 mL/10 g). The mice were placed in separate glass boxes. The writhing events of these animals were counted for 20 min. For scoring purposes, a writhing is defined as abdominal extension and simultaneous stretching of at least one hind limb<sup>19</sup>.

### Acknowledgments

This work was supported by grants from the National Natural Science Foundation of China (Nos. 21572274 and 21732008) and the CAMS Innovation Fund for Medical Sciences (No. 2016-I2M-1-010, China).

### Author contributions

Shishan Yu and Yong Li designed the study. Shihan Yu supervised the project. Yong Li, Yunbao Liu, Jing Qu, and Shuanggang Ma performed the bioassay-guided isolation, structure analysis, and discovered the analgesic compounds. Yuxun Zhu and Zhaoxin Zhang performed the antinociceptive tests. Li Li completed the ECD calculation. Shishan Yu and Yong Li wrote the paper. All authors contributed to the discussion and interpretation of the results.

### Conflicts of interest

The authors have no conflicts of interest to declare.

### Appendix A. Supporting information

Supporting data to this article can be found online at <https://doi.org/10.1016/j.apsb.2019.10.013>.

### References

1. Chen J, Zhen S. *Chinese poisonous plants*. Beijing: Science Press; 1987. p. 232.

- Li Y, Liu Y, Zhang J, Liu Y, Ma S, Qu J, Lv H, Yu S. Antinociceptive grayanoids from the roots of *Rhododendron molle*. *J Nat Prod* 2015; **78**:2887–95.
- Li Y, Liu Y, Yu S. Grayanoids from the Ericaceae family: structures, biological activities and mechanism of action. *Phytochem Rev* 2013; **12**:305–25.
- Li Y, Liu Y, Zhang J, Li Y, Jiang J, Yu S, Ma S, Qu J, Lv H. Mollolide A, a diterpenoid with a new 1,10:2,3-disecograyanane skeleton from the roots of *Rhododendron molle*. *Org Lett* 2013; **15**:3074–7.
- Li Y, Liu Y, Liu Y, Wang C, Wu L, Li L, Ma S, Qu J, Yu S. Mollanol A, a diterpenoid with a new C-nor-D-homograyanane skeleton from the fruits of *Rhododendron molle*. *Org Lett* 2014; **16**:4320–3.
- Li Y, Liu Y, Yan H, Liu Y, Li Y, Lv H, Ma S, Qu J, Yu S. Rhodomollins A and B, two diterpenoids with an unprecedented backbone from the fruits of *Rhododendron molle*. *Sci Rep* 2016; **6**:36752.
- Zhou J, Zhan G, Zhang H, Zhang Q, Li Y, Xue Y, Yao G. Rhodomollanol A, a highly oxygenated diterpenoid with a 5/7/5/5 tetracyclic carbon skeleton from the leaves of *Rhododendron molle*. *Org Lett* 2017; **19**:3935–8.
- Zhou J, Sun N, Zhang H, Zheng G, Liu J, Yao G. Rhodomollacetals A–C, PTP1B inhibitory diterpenoids with a 2,3:5,6-di-seco-grayanane skeleton from the leaves of *Rhododendron molle*. *Org Lett* 2017; **19**:5352–5.
- Zhou J, Liu J, Dang T, Zhou H, Zhang H, Yao G. Mollebenzylanol A and B, highly modified and functionalized diterpenoids with a 9-benzyl-8,10-dioxatricyclo [5.2.1.0<sup>1-5</sup>]decane core from *Rhododendron molle*. *Org Lett* 2018; **20**:2063–6.
- Lu Y, Raymond A. Absolute configuration of the antiinflammatory sponge natural product contignasterol. *J Nat Prod* 2002; **65**:1924–6.
- Liu J, Liu Y, Yan Y, Yang J, Lu X, Cheng Y. Commiphoratonones A and B, two sesquiterpene dimers from *Resina commiphora*. *Org Lett* 2018; **20**:2220–3.
- Li F, Zhan Z, Liu F, Yang Y, Li L, Feng Z, Jiang J, Zhang P. Polyflavanostilbene A, a new flavanol-fused stilbene glycoside from *Polygonum cuspidatum*. *Org Lett* 2013; **15**:674–7.
- Zhang M, Zhu Y, Zhan G, Shu P, Sa R, Lei L, Xiang M, Xue Y, Luo Z, Wan Q, Yao G, Zhang Y. Micranthanone A, a new diterpene with an unprecedented carbon skeleton from *Rhododendron micranthum*. *Org Lett* 2013; **15**:3094–7.
- Chen S, Zhang H, Wang L, Bao G, Qin G. Diterpenoids from the flowers of *Rhododendron molle*. *J Nat Prod* 2004; **67**:1903–6.
- Zhou S, Yao S, Tang C, Ke C, Li L, Lin G, Ye Y. Diterpenoids from the flowers of *Rhododendron molle*. *J Nat Prod* 2014; **77**:1185–92.
- Zhu Y, Zhang Z, Yan H, Lu D, Zhang H, Li L, Liu Y, Li Y. Antinociceptive diterpenoids from the leaves and twigs of *Rhododendron decorum*. *J Nat Prod* 2018; **81**:1183–92.
- Zhou J, Liu T, Zhang H, Zheng G, Qiu Y, Deng M, Zhang C, Yao G. Anti-inflammatory grayanane diterpenoids from the leaves of *Rhododendron molle*. *J Nat Prod* 2018; **81**:151–61.
- Burke J, Doskotch R, Ni C, Clardy J. Kalmanol, a pharmacologically active diterpenoid with a new ring skeleton from *Kalmia angustifolia* L. *J Am Chem Soc* 1989; **111**:5831–3.
- Guo Q, Xia H, Meng X, Shi G, Xu C, Zhu C, Zhang T, Shi J. *Acta Pharm Sin B* 2018; **8**:409–19.